Available online at www.sciencedirect.com

ScienceDirect

Procedia IUTAM 11 (2014) 110 – 118

Procedia IUTAM

www.elsevier.com/locate/procedia

Nonlinear Interfacial Wave Phenomena from the Micro- to the Macro-Scale

The conformal-mapping method for surface gravity waves in the presence of variable bathymetry and mean current

C. Viotti[a,*], D. Dutykh[a,b], F. Dias[a,c]

[a] *School of Mathematical Sciences, University College Dublin, Ireland*
[b] *CNRS and University of Savoie*
[c] *ENS Cachan*

Abstract

The conformal mapping formulation for the free-surface Euler equations in the presence of non homogeneous, yet stationary bathymetry is here derived and numerically implemented. The differences arising with respect to the more familiar flat-bottom and deep-water versions of the method are examined in detail. It is also shown how the loss of translational invariance due to the variable bottom profile naturally leads to consider a further extension of the method, which accounts for the superposition—otherwise immaterial—of an irrotational mean stream. As it is illustrated by numerical examples, the formulation presented is suitable for the study of fully nonlinear wave-topography and wave-current interactions realized by combining mean current and variable bathymetry.

Selection and peer-review under responsibility of scientific committee of Nonlinear Interfacial Wave Phenomena from the Micro- to the Macro-Scale

Keywords: Surface gravity waves; conformal mapping; spectral methods.

1. Introduction

The conformal mapping formulation for fully nonlinear surface waves in deep water and uniform finite depth, originally introduced by Dyachenko *et al.*[1], is described and analyzed in several papers (e.g., Choi & Camassa[2] and Li *et al.*[3]). A major advantage of such a formulation consists in its optimal viability for implementing efficient and accurate numerical schemes. While the method is notoriously limited to two spatial dimensions, it is still suitable to extension along different directions. In this regard, we mention the formulation for surface waves over a uniform shear current by Choi[4], and the perturbative weakly-three-dimensional extension by Ruban[5]. The conformal mapping approach has also been applied to the case of non-uniform bathymetry. In the earlier studies (e.g., Matsuno[6]), the method was employed mostly as an analytical tool for deriving asymptotic models for nonlinear wave evolution. More recently, Ruban[7,8] has considered the extension of the conformal mapping method to general and even time-dependent bathymetry profiles as an approach to numerical simulation. In this paper we aim to provide a more direct derivation of the transformed dynamical system, which parallels the formulation most commonly adopted in regard

* Corresponding author.
E-mail address: claudio.viotti@ucd.ie

Selection and peer-review under responsibility of scientific committee of Nonlinear Interfacial Wave Phenomena from the Micro- to the Macro-Scale
doi:10.1016/j.piutam.2014.01.053

to the the flat-bottom and deep-water cases [9,3,2], and is suitable for emphasizing particular aspects of the numerical implementation. We also propose a further extension of the approach to account for the presence of a non-uniform irrotational current. While a few fully-nonlinear numerical studies [10,11] of the wave-current interaction have been performed by means of different numerical approaches (boundary elements method), we are not aware of any existing generalization of the conformal-mapping method along this direction.

To begin with, we define the problem and introduce the basic governing equations. By assuming irrotational flow, and neglecting surface tension effects (which however can be included in a straightforward way, see for instance Milewski *et al.* [9]), the free-surface Euler equations in two spatial coordinates (x, y) and time t read

$$\begin{aligned} &\nabla^2\phi = 0, && \text{for} \quad b(x) < y < \zeta(x,t), \quad 0 < x < L \\ &\left.\begin{aligned} &\zeta_t = -\phi_x\zeta_x + \phi_y, \\ &\phi_t = -\frac{1}{2}\left(\phi_x{}^2 + \phi_y{}^2\right) - g\zeta, \end{aligned}\right\} && \text{at} \quad y = \zeta(x,t) \\ &\nabla\phi\cdot\mathbf{n} = 0, && \text{at} \quad y = b(x) \end{aligned} \tag{1}$$

where $\zeta(x,t)$ is the free surface elevation, $\phi(x,y,t)$ the velocity potential, $b(x) < 0$ the bottom profile, and g is the vertical acceleration due to gravity. The fluid density is assumed here to be unitary without loss of generality, also, non dimensional units in which g and a characteristic depth scale are equal to one will be understood. As we shall solve numerically the above equations by means of a spectral method, we assume from the outset periodic boundary conditions in the horizontal direction x. This implies that ζ and $\nabla\phi$ (the velocity of the fluid) are periodic functions, whereas ϕ is not necessarily so. We stress, however, that the following mathematical derivation applies to the free-space conditions without any substantial modification.

2. Mathematical formulation

2.0.1. The conformal mapping

The first step to formulating the free-surface system (1) in the conformal space consists in finding the analytic transformation $Z = X(\xi,\eta,t) + iY(\xi,\eta,t)$ that maps the physical domain filled by the fluid into a strip of uniform thickness $\overline{h} > 0$, where so far the choice of $\overline{h}$ can be considered arbitrary. The vertical displacement of the free surface and the known bathymetry profile provide both boundary conditions for the function Y

$$Y(\xi,0,t) = y(\xi,t), \quad Y(\xi,-\overline{h},t) = h(\xi,t),$$

whereas the boundary conditions for X,

$$X(\xi,0,t) = x(\xi,t), \quad X(\xi,-\overline{h},t) = \chi(\xi,t),$$

must be determined. Note that $\overline{h}$, which represents the bathymetry profile in the conformal space, is allowed to depend on time even though the physical bottom geometry is steady. As it will be better clarified in the following, this fact stems from the very nature of the conformal mapping, which depends on the configuration of the free surface at given time.

We shall assume ξ-periodic solutions of period $\ell = 2\pi/k_0$ in the transformed plane. The boundary conditions for Y can then be expanded in Fourier series

$$Y(\xi,0,t) = y(\xi,t) = \sum_n \hat{Y}_n e^{ink_0\xi}, \tag{2}$$

$$Y(\xi,-\overline{h},t) = h(\xi,t) = \sum_n \hat{H}_n e^{ink_0\xi}, \tag{3}$$

and it is easy to verify that the most general harmonic function satisfying the above conditions has the form

$$Y = -\eta\frac{\hat{H}_0}{\overline{h}} + \hat{Y}_0\left(1+\frac{\eta}{\overline{h}}\right) + {\sum_n}' \hat{Y}_n \frac{\sinh nk_0(\eta+\overline{h})}{\sinh nk_0\overline{h}} e^{ink_0\xi} + {\sum_n}' \hat{H}_n \frac{\sinh nk_0\eta}{\sinh nk_0\overline{h}} e^{ink_0\xi}, \tag{4}$$

where $\sum_n'$ denotes summation over integers except for $n = 0$. From the Cauchy–Riemann conditions, $X_\xi = Y_\eta$ and $X_\eta = -Y_\xi$, one obtains the relations

$$x_\xi(\xi,t) = -\frac{\hat{H}_0}{\overline{h}} + \hat{Y}_0\frac{1}{\overline{h}} + \sum_n{}' \hat{Y}_n nk_0 \coth nk_0\overline{h} e^{ink_0\xi} - \sum_n{}' \hat{H}_n \frac{nk_0}{\sinh nk_0\overline{h}} e^{ink_0\xi}, \tag{5}$$

$$\chi_\xi(\xi,t) = -\frac{\hat{H}_0}{\overline{h}} + \hat{Y}_0\frac{1}{\overline{h}} + \sum_n{}' \hat{Y}_n \frac{nk_0}{\sinh nk_0\overline{h}} e^{ink_0\xi} - \sum_n{}' \hat{H}_n nk_0 \coth nk_0\overline{h} e^{ink_0\xi}. \tag{6}$$

One can observe that by setting $\overline{h} = \hat{Y}_0 - \hat{H}_0$ the first coefficient of the above Fourier expansions becomes equal to 1, whereby the spatial period results to be the same in both conformal and physical space, i.e., $\ell = L$. Note that, in doing so, $\overline{h}$ is time-dependent. One integration of (5) and (6) with respect to ξ allows to obtain X as

$$X = x_0(t) + \xi - \sum_n{}' \mathrm{i}\hat{\mathrm{Y}}_\mathrm{n} \frac{\cosh \mathrm{nk}_0(\eta+\overline{\mathrm{h}})}{\sinh \mathrm{nk}_0\overline{\mathrm{h}}} \mathrm{e}^{\mathrm{ink}_0\xi} + \sum_\mathrm{n}{}' \mathrm{i}\hat{\mathrm{H}}_\mathrm{n} \frac{\cosh \mathrm{nk}_0\eta}{\sinh \mathrm{nk}_0\overline{\mathrm{h}}} \mathrm{e}^{\mathrm{ink}_0\xi}.$$

where x_0 is an integration constant which determines the origin of the coordinate system in physical space. Even though it seems natural to require x_0 to be constant, it is convenient to keep this quantity undetermined for the time being and defer its determination to a later stage.

The velocity potential, Φ, and the streamfunction, Ψ, also constitute a harmonic-conjugate pair, which is subject to the boundary conditions

$$\Phi(\xi,0,t) = \phi(\xi,t), \quad \Psi(\xi,-\overline{h},t) = Q(t). \tag{7}$$

The above boundary conditions are insufficient to close either one of the two Laplace problems for Φ and Ψ individually, however, the Cauchy–Riemann relations determine a unique solution of the two problems as a pair. Note that, since the trace of the stream function on the free surface $\Psi(\xi,0,t) = \psi(\xi,t)$ is to be determined as part of the solution, the constant Q has no physical relevance and can be set equal to zero without loss of generality. As mentioned above, the velocity potential is not periodic in general, but its periodic part can be written as

$$\phi(\xi,t) - \mathcal{U}\xi = \sum_n{}' \hat{C}_n e^{ink_0\xi}. \tag{8}$$

where $\mathcal{U}$ represent the mean horizontal velocity of the flow. By the Cauchy–Riemann relations, the $\mathcal{U}\xi$ component of ϕ must correspond to the physically meaningful difference between the mean values of the streamfunction at the free surface and bottom, namely

$$\mathcal{U}\overline{h} = m[\psi],$$

where the operator $m[\cdot]$ denotes the average over one period

$$m[f] = \frac{1}{\ell}\int_0^\ell f(\xi)\mathrm{d}\xi.$$

Following the same procedure as for (X, Y) one obtains

$$\Phi = \mathcal{U}\xi + \sum_n{}' \hat{C}_n \frac{\cosh nk_0(\eta+\overline{h})}{\cosh nk_0\overline{h}} e^{ink_0\xi}, \tag{9}$$

$$\Psi = \mathcal{U}(\eta+\overline{h}) + \sum_n{}' \hat{C}_n \frac{\mathrm{i}\sinh \mathrm{nk}_0(\eta+\overline{\mathrm{h}})}{\cosh nk_0\overline{h}} e^{ink_0\xi}, \tag{10}$$

and, on the free surface,

$$\psi(\xi,t) - \mathcal{U}\overline{h} = \sum_n{}' i\hat{C}_n \tanh nk_0 e^{ink_0\xi}. \tag{11}$$

Note how the above relations are the same as for the flat-bottom case (cf. Choi & Camassa[2]), as the boundary conditions (7) are independent of the bottom geometry. In the presence of an uneven bottom, however, the system is

not Galilean invariant, whereby the effect of $\mathcal{U}$ does not reduce to a simple Galilean boost, as we shall discuss later. We also emphasize that a uniform stream in the conformal space is not preserved by the conformal mapping, whereas it conserves the same potential jump across one domain period in physical space.

We next introduce the operators that generalize the familiar Hilbert-transform-like operators arising in the deep-water and flat-bottom formulations to express the relations between x and y as well as ϕ and ψ in a compact form (which also allow the extension of the formalism to non-periodic solutions). Since the Fourier symbols of the transformations are all contained in the above expressions (5), (6) and (11), the corresponding operators can be obtained by using the convolution theorem:

$$\mathscr{T}_x[f,g] = \frac{1}{\overline{h}} \fint f(\xi') \coth[\pi(\xi'-\xi)/2\overline{h}]\mathrm{d}\xi' + \frac{1}{\overline{h}} \fint (g(\xi')-\overline{h}) \tanh[\pi(\xi'-\xi)/2\overline{h}]\mathrm{d}\xi', \tag{12}$$

$$\mathscr{T}_y[f,g] = \frac{1}{\overline{h}} \fint f(\xi') \mathrm{cosech}[\pi(\xi'-\xi)/2\overline{h}]\mathrm{d}\xi' + \frac{1}{\overline{h}} \fint (g(\xi')-\overline{h}) \mathrm{sech}[\pi(\xi'-\xi)/2\overline{h}]\mathrm{d}\xi', \tag{13}$$

$$\mathscr{T}_s[f] = -\frac{1}{\overline{h}} \fint f(\xi') \mathrm{cosech}[\pi(\xi'-\xi)/2\overline{h}]\mathrm{d}\xi', \tag{14}$$

where $\fint$ denotes the principal-value integral over the real axis. Note that the operator $\mathscr{T}_y$ is the inverse of $\mathscr{T}_x$ with respect to the first argument, i.e., $\mathscr{T}_y[\,\cdot\,,g] = \mathscr{T}_x^{-1}[\,\cdot\,,g]$. In terms of integral operators, relations (5) and (6) can then be written as

$$x_\xi = 1 - \mathscr{T}_x[y_\xi, h_\xi], \tag{15}$$

$$\chi_\xi = 1 + \mathscr{T}_x[h_\xi, y_\xi], \tag{16}$$

$$y_\xi = \mathscr{T}_y[x_\xi - 1, h_\xi], \tag{17}$$

while the relations between x and y reads

$$x = x_0(t) + \xi - \mathscr{T}_x[y,h]. \tag{18}$$

Note that the bathymetry profile in the conformal space is $h = b(\chi(\xi,t))$, whereby all of the above transformations contain an implicit, nonlinear dependence on the current configuration of the free surface. This fact implies that $h(\xi,t)$ must be determined beforehand at any time t in such a way to match the physical bottom profile. This task can be handled by numerical iterations (see § 3).

Finally, we write in compact notation the relations connecting potential and streamfunction as

$$\phi_\xi = -\mathscr{T}_s[\psi_\xi] + \mathcal{U}, \quad \psi_\xi = -\mathscr{T}_s[\phi_\xi - \mathcal{U}].$$

2.0.2. Governing equations in conformal space

Following Choi & Camassa, the governing equations in the conformal space are obtained by transforming the physical-space equations by chain-rule differentiation. While such a process may appear overall straightforward, some elements of it need careful explanation in connection with the present generalization. The transformed kinematic equation for the free surface (the first equation in (1)) reads

$$y_t x_\xi - x_t y_\xi = -\psi_\xi, \tag{19}$$

which also can be written as

$$\mathrm{Im}\left(\frac{z_t}{z_\xi}\right) = -\frac{\psi_\xi}{J},$$

where $z = Z(\xi,0,t) = x + \mathrm{i}y$. The real part of Z_t/Z' can be related to its imaginary part by the same procedure as for (X,Y), but only once $\mathrm{Im}\,(Z_t/Z')$ at the bottom has been determined. Such information is obtained by transforming the kinematic condition at the bottom, i.e., $h_t = 0$, as previously done for the kinematic condition at the free suface. In doing so, one obtains

$$\mathrm{Im}\left(\frac{Z_t}{Z'}\right) = \overline{h}_t, \qquad \text{at} \quad \eta = -\overline{h}.$$

Since the harmonic-conjugate pair $(\mathrm{Re}(Z_t/Z'), \mathrm{Im}(Z_t/Z'))$ is subject to the same kind of boundary conditions as (X, Y), an analogous relation holds between its real and imaginary part on the free surface:

$$\mathrm{Re}\left(\frac{z_t}{z_\xi}\right) = \frac{y_t y_\xi + x_t x_\xi}{J} = \mathscr{T}_x\left[\frac{\psi_\xi}{J}, \overline{h}_t\right] + q(t). \tag{20}$$

Since the quantity $\overline{h}_t$, appearing as the second argument of $\mathscr{T}_x[\cdot,\cdot]$, does not depend on ξ, it only produces a constant value. One can therefore replace it with zero and absorb the effect of $\overline{h}_t$ in the definition of $q(t)$. For this reason we shall use the short-hand $\mathscr{T}_x[a] \equiv \mathscr{T}_x[a, 0]$ in what follows.

By solving equations (19) and (20) for x_t and y_t one obtains

$$x_t = x_\xi \mathscr{T}_x\left[\frac{\psi_\xi}{J}\right] + x_\xi q(t) + y_\xi\left(\frac{\psi_\xi}{J}\right), \tag{21}$$

$$y_t = -x_\xi\left(\frac{\psi_\xi}{J}\right) + y_\xi \mathscr{T}_x\left[\frac{\psi_\xi}{J}\right] + y_\xi q(t). \tag{22}$$

Equation (21) shows that the constant $q(t)$ is related to $x_0(t)$, whereby the choice of either one of such constants determines the other. In the presence of variable bathymetry the most natural choice consists in requiring that $x_0 = const.$. By noting that $m(x_\xi) = 1$ this is accomplished by setting

$$q(t) = m\left(x_\xi \mathscr{T}_x\left[\frac{\psi_\xi}{J}\right] + y_\xi\left(\frac{\psi_\xi}{J}\right)\right),$$

which allows the term $x_\xi q(t)$ to absorb the mean value of the right-hand side of equation (21), i.e., x_{0_t}.

By use of (19) and (20) the dynamic condition at the free surface can be written as

$$\phi_t = -\frac{1}{J}\left[\frac{1}{2}\phi_\xi^2 - \frac{1}{2}\psi_\xi^2 - J\phi_\xi \mathscr{T}_x(\psi_\xi/J)\right] - gy + C(t), \tag{23}$$

which differs from the equation that holds for uniform depth (cf. Choi & Camassa[2] equation (35)) only by the definition of the integral operator $\mathscr{T}_x$.

So far we have assumed periodic wave motion, which does not imply ϕ is a periodic function itself. While ϕ may still be made periodic in principle, this choice would result in a "saw-tooth"-like function, unsuitable for a spectral numerical implementation due to the well-known Gibbs phenomenon. The function $\varphi = \phi(\xi, t) - \mathcal{U}\xi$, on the other hand, is periodic, as shown by equation (8). By looking at the right-hand side of equation (23), one can realize that all terms appearing in it are periodic in ξ, due to the fact that ϕ appears always as a derivative. The time evolution can therefore affect the periodic part of the potential φ only, implying that $\mathcal{U}$ is a constant of motion. We can then easily derive an evolution equation for φ only by substituting $\phi = \varphi - \mathcal{U}\xi$ into (23) and bearing in mind the last observation:

$$\varphi_t = -\frac{1}{J}\left[\frac{1}{2}(\varphi_\xi + \mathcal{U})^2 - \frac{1}{2}\psi_\xi^2 - J(\varphi_\xi + \mathcal{U})\mathscr{T}_x\left(\frac{\psi_\xi}{J}\right)\right] - gy + C(t), \tag{24}$$

where $\mathcal{U}$ appears as a parameter.

The explicit appearance of $\mathcal{U}$ inside the above evolution equation makes its physical relevance apparent, as anticipated in the previous section. Furthermore, since ϕ is a periodic function the above equation is suitable for numerical solution by spectral methods. This second formulation is a convenient way of taking into account for the effect of a mean stream, whose intensity is tuned by the parameter $\mathcal{U}$.

3. Numerical computations

A pseudo-spectral method is employed for solving the evolution equations (22) and (23) under periodic boundary conditions. The discretization based on Discrete Fourier Transform is a standard procedure which we do not intend to comment on, as for the time integration of the resulting system of ordinary differential equations for the Fourier coefficients we use an adaptive solver available in many common software packages.

As we anticipated, the major complexity introduced by the variable bathymetry consists in the need to update the bottom profile $h(\xi, t)$, which depends on both the physical bathymetry and the instantaneous surface elevation $y(\xi, t)$, before any evaluation of the right-hand side. Fixed-point iterations can be used to update $h(\xi, t)$ starting from an initial estimate $h^{(0)}$ provided by the most recent value of such function (obtained from the previous time step). A single fixed-point iteration consists of

$$\chi^{(n)} = \xi - \mathscr{T}_x[y(\xi), h^{(n)}(\xi)], \tag{25}$$

$$h^{(n+1)} = b(\chi^{(n)}), \tag{26}$$

and the arresting criterion in based on the condition that the residue $R^{(n)} = \|H(\chi^{(n)}) - H(x)\|$ has decreased below a fixed tolerance τ_R, for a suitable norm $\|\cdot\|$. In what follows we use $\|\cdot\| = \|\cdot\|_\infty$. We remark that basic fixed-point iterations only converge linearly, i.e., $R^{(n+1)} \approx CR^{(n)}$ for $|C| < 1$, and that in the presence of strong bathymetric variations the convergence factor C was found to degrade (i.e., become close to 1) quite dramatically. In such cases the iterative process can become computational heavy. While this fact points to the need for implementing an optimized iteration scheme we shall leave this task to forthcoming work.

3.1. Soliton fission over submerged step

The bathymetry $b(x)$ employed in this example consists of a "plateau" reaching the height $H = 0.4$ with respect to the flat ground level of depth $h_0 = 1$ (see figure 1):

$$b(x) = -h_0 + \frac{H}{2}\tanh\left(\frac{x - x_1}{\delta}\right) - \frac{H}{2}\tanh\left(\frac{x - x_2}{\delta}\right).$$

where x_1 and x_2 denote the two edges of the bottom elevation. A right-propagating solitary wave is precomputed for flat bottom of unitary depth, and placed upstream of the first depth variation at $x = x_1$. The evolution ensuing from the interaction with the underwater step is shown in figure 1. The solitary wave propagates undisturbed until it reaches the depth transition. The following dynamics is characterized by a fission of the incoming wave into a pair of solitons with different magnitudes, which then keep separating due to the different propagation speed. A small reflected wave is also generated during the soliton-step interaction.

In order to assess the accuracy of the numerical solution, we show in figure 2 the precision attained on the conservation of total mass M and energy E. In these plots we report results corresponding to different values of the tolerance τ_R, with all other parameters held constant. As we have employed a large number of Fourier modes and imposed a stringent error tolerance accuracy in the time-stepping routine, we can expect the run-time update of the bathymetry profile h to dominate the numerical error for a wide range of values of τ_R. As it can be seen in figure 2, the numerical error, which mostly accumulates during the stage of soliton-step interaction, scales well with respect to τ_R up to $\tau_R = 10^{-8}$. Any decrease of τ_R below $\tau_R \approx 10^{-8}$ does not further improve the numerical accuracy, indicating that the computation of the bathymetry profile is no longer the dominant source of numerical error. The typical number of iterations required in the cases above consists of 6 (for $\tau_R = 10^{-10}$), 3 (for $\tau_R = 10^{-8}$) , 1 (for $\tau_R = 10^{-6}$), and only sparse single iterations for larger tolerance values. We remark again that the results just discussed, which are reported here to illustrate the behavior of the numerical method, can be strongly affected by the particular bathymetry employed.

3.2. Supercritical stream over submerged obstacle

The second case we present consists of a uniform stream flowing over a submerged hump. The stationary solution to this problem, for the case of a triangular obstacle, was solved and analyzed by means of conformal mapping by Dias & Vanden-Broeck [12], who found a family of stationary solutions in a range of obstacle height and Froude number Fr. For any supercritical flow (Fr > 1) such stationary solutions can be thought of as a family of forced solitary waves anchored over the obstacle, which tend to classic, unforced solitary waves as the amplitude of the obstacle vanishes, provided $1 < \mathrm{Fr} < 1.2942$ (the range of existence of solitary waves). In this example, we consider an initial condition which consists of a flat surface, $\eta(x, 0) = 0$, and a uniform current introduced by setting $\phi(\xi, 0) = \mathcal{U}\xi$.

Other previous studies have investigated analytically and numerically the stability of analogous steady waves generated by localized submerged obstacles in the framework of KdV dynamics [13,14]. The bottom variation was represented

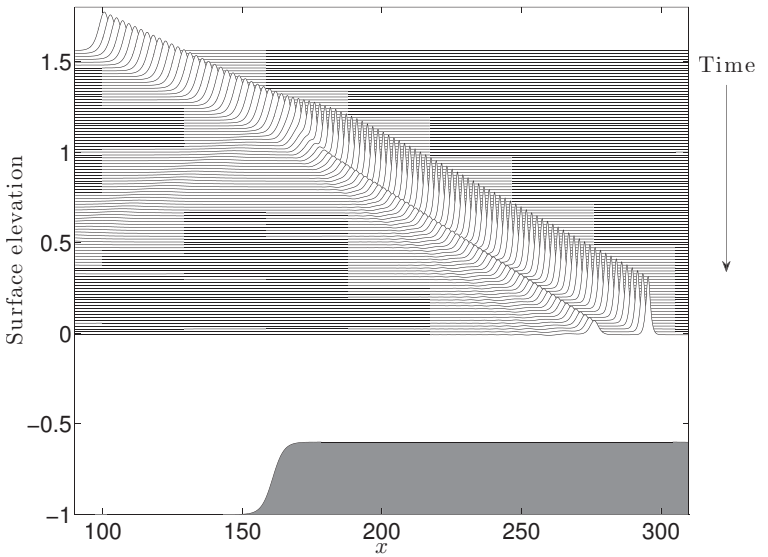

Figure 1. Time evolution of a solitary wave propagating over a strong depth variation (only a part of the x-period is shown). The initial speed of the soliton is $c_s = 1.1$ (with $c_0 \equiv \sqrt{gh_0} = 1$). Frames are shown from $t = 0$ up to $t = 200$, time increases from top to bottom in order to better show details. For this simulation we employ 16384 dealiased Fourier modes for the total domain size $L = 256\pi$.

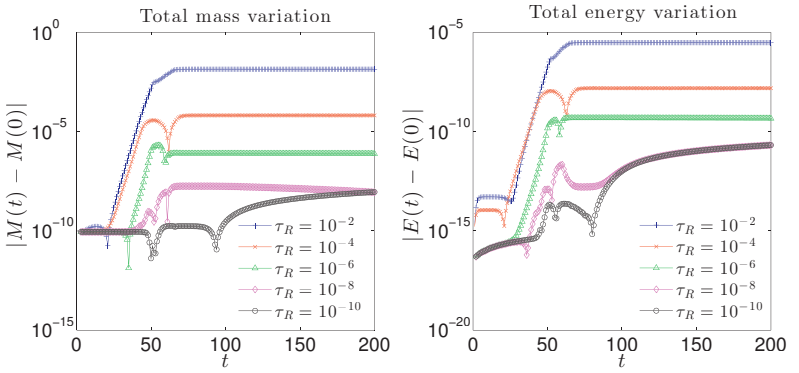

Figure 2. Variation in time of the total mass and total energy for the simulation shown in figure 1 and for different values of the tolerance τ_R set in the run-time update of $h(\xi, t)$.

in those studies by introducing an equivalent forcing term in the evolution equations, nonetheless the available results can be used as a reference for assessing the qualitative features of fully nonlinear dynamics. In the supercritical regime such steady wave solutions are found to be very stable, meaning that even strong perturbations are invariably shed away by the current leaving the steady solution unaffected. The fully nonlinear computation that we perform with the present approach shows a similar behavior. As shown in figure 3 a steady wave solution is recovered over the obstacle after a transient emission of radiation. This case is close to the stable supercritical solution computed by Camassa & Wu [14] (see figure 16 in that paper), with the most visible difference consisting of a right-propagating soliton that separates from the radiated wave packet not present in the KdV simulation.

Another important aspect of the flow evolution consists in the wave resistance associated with the release of radiative waves. The wave resistance can be identified with the time derivative of the total horizontal momentum $P_x(t)$ (see figure 4). Consistently, once again, with the measurement of wave resistance presented by Camassa & Wu, the curve $P_x(t)$ starts flat at $t = 0$ then monotonically decreases until it stabilizes on a constant value. An inflection point is present at $t \sim 5$, which correspond to the time of maximum wave resistance.

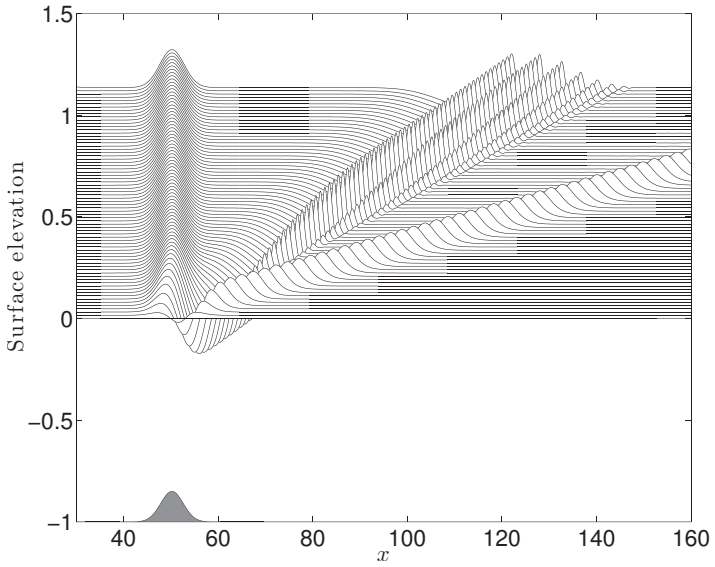

Figure 3. Time evolution of the initially flat free surface due to a current flowing over a submerged Gaussian-shaped obstacle. The Froude number is Fr = 2 (corresponding to $\mathcal{U} = 2$), the protrusion of the obstacle is 0.25. Frames are shown from $t = 0$ every 4 time units.

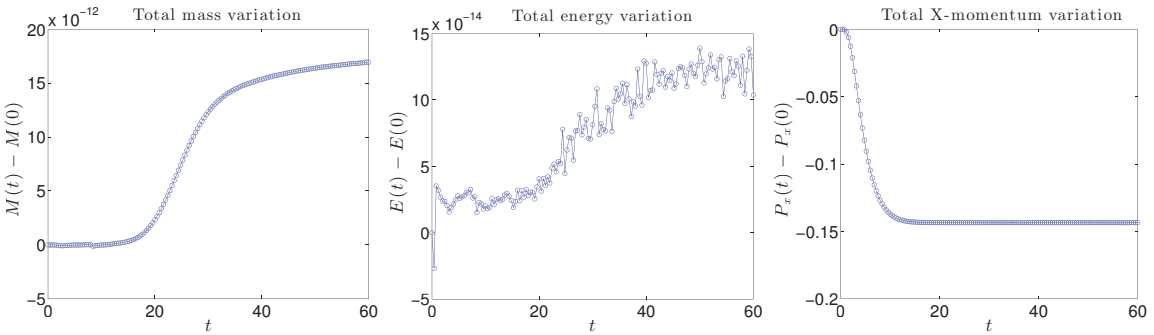

Figure 4. Variation in time of the total mass M, energy E, and horizontal momentum P_x, for the simulation shown in figure 3.

4. Concluding remarks

We have presented the conformal mapping formulation for the two-dimensional free-surface Euler equations over a non-uniform bathymetry, and we have discussed a criterion for including also the effect of an irrotational mean current. The overall mathematical structure is maintained analogous to the deep-water and flat-bottom cases, as the effect of the non-uniform bathymetry is conveniently contained in the Hilbert-transform-like operators that link harmonic-conjugate quantities. From the point of view of the numerical implementation, the major complication arises from the need to update the bathymetric profile in the conformal space due to the evolution of the free surface. We have solved this problem by means of fixed-point iterations, and we have presented numerical examples, based on the pseudo-spectral discretization, in which the solution was resolved at nearly machine-precision accuracy. The method is suitable to generalization to time-dependent bottom bathymetry.

Acknowledgements

This publication has emanated from research conducted with the financial support of European Research Council under the research project ERC-2011-AdG 290562-MULTIWAVE and Science Foundation Ireland under Grant Number SFI/12/ERC/E2227.

References

1. A. L. Dyachenko, V. E. Zakharov, and E. A. Kuznetsov. Nonlinear dynamics on the free surface of an ideal fluid. *Plasma Phys. Rep.*, 22:916–928, 1996.
2. W. Choi and R. Camassa. Exact evolution equations for surface waves. *J. Eng. Mech.*, 125:756–760, 1999.
3. Y. A. Li, J. M. Hyman, and W. Choi. A numerical study of the exact evolution equations for surface waves in water of finite depth. *Stud. Appl. Maths*, 113:303–324, 2004.
4. W. Choi. Nonlinear surface waves interacting with a linear shear current. *Mathematics and Computers in Simulation*, 80:29–36, 2009.
5. V.P. Ruban. Conformal variables in the numerical simulations of long-crested rogue waves. *Eur. Phys. J. Spec. Top.*, 185, 2010.
6. Y. Matsuno. Nonlinear evolution of surface gravity waves over an uneven bottom. *J. Fluid Mech.*, 249:121–133, 1993.
7. V.P. Ruban. Water waves over a time-dependent bottom: Exact description for 2D potential flow. *Phys. Lett. A*, 340:194–200, 2005.
8. V.P. Ruban. Water waves over a strongly undulanting bottom. *Phys. Rev. E*, 70:066302, 2004.
9. P. A. Milewski, J.-M. Vanden-Broeck, and Z. Wang. Dynamics of steep two-dimensional gravity-capillary solitary waves. *J. Fluid Mech.*, 664:466–477, 2010.
10. D. Ning, X. Zhou, T. Hou, and B. Teng. Numerical investigation of focused waves on uniform currents. *Proc. 22nd International Offshore and Polar Engineering Conference*, 2012.
11. M. H. Kim, M.S. Celebi, and D.J. Kim. Fully nonlinear interactions of waves with a three-dimensional body in uniform currents. *Appl. Ocean Res.*, 20:309–321, 1998.
12. F. Dias and J.-M. Vanden-Broeck. Open channel flows with submerged obstructions. *J. Fluid Mech.*, 206:155–170, 1989.
13. F. Chardard, F. Dias, H. Y. Nguyen, and J.-M. Vanden-Broeck. Stability of some stationary solution to the forced KdV equation with one or two bumps. *J. Eng. Math.*, 70:175–189, 2011.
14. R. Camassa and T. J. Wu. Stability of forced steady solitary waves. *Phil. Trans. Royal Soc. London A*, 337:429–466, 1991.